Available online at www.sciencedirect.com
SCIENCE DIRECT®
Combustion and Flame 145 (2006) 316–323
Combustion and Flame
www.elsevier.com/locate/combustflame

Testing a small detailed chemical-kinetic mechanism for the combustion of hydrogen and carbon monoxide

Priyank Saxena *, Forman A. Williams

Center of Energy Research, Department of Mechanical and Aerospace Engineering, University of California, San Diego, La Jolla, CA 92093, USA

Received 19 May 2005; received in revised form 2 October 2005; accepted 12 October 2005

Available online 15 November 2005

Abstract

A relatively small detailed mechanism has been developed for the combustion of various fuels, mainly hydrocarbons, in air or oxygen-inert mixtures. This mechanism has been tested previously for autoignition, premixed-flame burning velocities, and structures and extinction of diffusion flames and of partially premixed flames of many of these fuels. While submechanisms for hydrogen and carbon monoxide are essential components of this mechanism, thorough testing of the predictions of the mechanism for these simpler fuels has not been performed recently. Such testing is reported here and leads to modifications of rate parameters for a few of the most important elementary steps, as well as to deletion of one reaction and addition of another.

Keywords: Chemical-kinetic mechanisms; Autoignition; Laminar burning velocities; Diffusion-flame extinction; Hydrogen; Carbon monoxide

1. Introduction

Because of limitations on computer capabilities, there is a need for detailed chemical-kinetic mechanisms for combustion that are not too large. As an alternative to mechanisms having thousands of elementary steps, a mechanism having less than 300 steps is being developed [1]. This simplification is achieved by restricting attention to temperatures above about 1000 K, pressures below about 100 bar, equivalence ratios less than about 3 in premixed systems, and strain rates greater than about 50 s^{-1} in nonpremixed or partially premixed systems. The simplifications then arise mainly from the unimportance of soot formation and cool-flame phenomena under these conditions.

Fuels that have been studied previously with this mechanism include methane [2], ethane [3], ethylene [4], acetylene [5,6], propane [1], propene [1], propyne [1], allene [1], and methanol [7,8]. Tests also have been made recently for hydrogen autoignition [9], and some time ago premixed and diffusion flames of carbon monoxide were addressed [10,11]. There have, however, been no recent tests for premixed hydrogen flames and no tests at all for autoignition of mixtures containing carbon monoxide. Since the hydrogen and carbon monoxide submechanisms are essential to the mechanisms of all of the other fuels, and since there is also substantial interest in these two fuels them-

* Corresponding author. Fax: +1 (858) 534 5354.
E-mail address: psaxena@ucsd.edu (P. Saxena).

0010-2180/$ – see front matter
doi:10.1016/j.combustflame.2005.10.004

selves, testing of the mechanism for them is completed here.

Results from the present work on the submechanism for hydrogen and carbon monoxide are included in the larger mechanism that extends through propane [1]. The comparisons to be reported lead to small revisions of rate parameters for a few elementary steps. The resulting steps and rate parameters for this submechanism are given in Table 1, in which all steps are considered to be reversible, with backward rates obtained from listed forward rates by use of equilibrium constants. The revisions improve agreements in the present comparisons, for the most part without significantly affecting previous comparisons for methane, ethane, ethylene, and acetylene. The revised values are in agreement with those in some of the more recent literature, and the changes are well within fundamental uncertainties in rates of elementary steps. These uncertainties were considered for all of the steps, and possibilities of revising rate parameters for many additional steps were investigated but finally rejected as insufficiently useful or not justified well enough from fundamental considerations. In addition, one reaction is deleted that has been demonstrated recently to be unlikely to occur, and one has been added that previously had been thought to be unimportant but was found to exert a small but noticeable effect.

In the following sections comparisons are made first for premixed hydrogen systems, next for hydrogen diffusion-flame extinction, then for burning velocities of premixed flames of carbon monoxide with different amounts of hydrogen, and finally for autoignition of mixtures of carbon monoxide and hydrogen. The rate-parameter revisions are discussed in connection with the test for which they are most relevant. The computations for the comparisons were performed with CHEMKIN [19] programs, although the FLAMEMaster program [20] was also employed to make sure that predictions from the two different programs were the same.

2. Hydrogen burning velocities

There is a wealth of data available for laminar flame speeds for hydrogen–air systems for a wide range of equivalence ratios at normal atmospheric pressure and initially room temperature. In the earliest predecessor of the present mechanism for hydrogen [21], comparisons were made with data taken prior to 1990. These results exhibited a great deal of scatter, but more recent data are much more accurate. The measurements that we judge to be most reliable were selected for comparisons in the present work. These include hydrogen–air data at 1 atm and an initial temperature of 298 K for equivalence-ratio ranges of 0.23 to 4.5 [22], 0.25 to 1.5 [23], 0.4 to 4.0 [24], and 0.6 to 4.5 [25]. These results are in remarkably good agreement with each other. In addition, for these same conditions good data are available [25] for hydrogen–oxygen mixtures diluted by argon and by helium at 1 atm, and also [24] at pressures up to 20 atm for this last diluent.

Figs. 1 and 2 compare the present burning-velocity predictions with these data. The computational results were obtained with CHEMKIN 3.7 PREMIX including multicomponent diffusion and Soret effects but excluding radiant energy loss, which would decrease predicted burning velocities only slightly under these conditions. Throughout the present work, calculations also were made including radiant loss from H_2O and CO_2 bands in an optically thin approximation, and results differed approximately by the thickness of the lines.

A dilution factor may be defined as

$$f = [O_2]/\big([O_2] + [I]\big),$$

where the brackets denote concentrations and I stands for the inert; $f = 0.214$ in Fig. 1, and $f = 0.08$ in Fig. 2. The agreements between predictions and experiments are quite good in these figures, comparable with the agreements obtained previously [26] by a more complex mechanism. Although measured burning velocities in air for very lean mixtures consistently exceed predictions, the exceptionally strong tendency toward forming cellular flames under these conditions makes experiments very difficult and would tend to produce measured burning velocities that are higher than those of a planar, unstretched flame, to which the computations apply.

The small mechanism originally had 22 elementary steps for hydrogen combustion, but recent calculations of potential–energy surfaces [27] show clearly that one of the two chain-initiation steps that had been included, namely $H_2 + O_2 \rightarrow 2OH$, is highly unlikely, leaving only the reverse of step 12, $H_2 + O_2 \rightarrow HO_2 + H$, for initiation. The unlikely step therefore now is deleted. Although this step influenced autoignition times at higher temperatures, coupled with the other rate-parameter modifications indicated below, its deletion does not degrade reported [9] ignition-time comparisons. The comparisons in Figs. 1 and 2 therefore pertain to a 21-step hydrogen combustion mechanism, the first 21 entries in Table 1.

When the mechanism was first tested against these data, it gave burning velocities noticeably higher than those shown in Fig. 1 for air over most of the equivalence-ratio range and much lower than shown in Fig. 2. The rate parameters therefore were reviewed

Table 1
Chemical-kinetic mechanism for hydrogen and carbon monoxide

Reaction		A[a]	n[a]	E[a]	Reference
		Hydrogen–oxygen chain			
1. $H + O_2 \rightarrow OH + O$		3.52×10^{16}	−0.7	71.4	[12]
2. $H_2 + O \rightarrow OH + H$		5.06×10^{4}	2.7	26.3	[13]
3. $H_2 + OH \rightarrow H_2O + H$		1.17×10^{9}	1.3	15.2	[14]
4. $H_2O + O \rightarrow OH + OH$		7.60×10^{0}	3.8	53.4	[13]
		Direct recombination			
5.[b] $H + H + M \rightarrow H_2 + M$		1.30×10^{18}	−1.0	0.0	See text
6.[c] $H + OH + M \rightarrow H_2O + M$		4.00×10^{22}	−2.0	0.0	See text
7.[d] $O + O + M \rightarrow O_2 + M$		6.17×10^{15}	−0.5	0.0	See text
8.[e] $H + O + M \rightarrow OH + M$		4.71×10^{18}	−1.0	0.0	See text
9.[e] $O + OH + M \rightarrow HO_2 + M$		8.00×10^{15}	0.0	0.0	See text
		Hydroperoxyl reactions			
10.[f] $H + O_2 + M \rightarrow HO_2 + M$	k_0	5.75×10^{19}	−1.4	0.0	See text
	k_∞	4.65×10^{12}	0.4	0.0	
11. $HO_2 + H \rightarrow OH + OH$		7.08×10^{13}	0.0	1.2	[15]
12. $HO_2 + H \rightarrow H_2 + O_2$		1.66×10^{13}	0.0	3.4	[15]
13. $HO_2 + H \rightarrow H_2O + O$		3.10×10^{13}	0.0	7.2	[16]
14. $HO_2 + O \rightarrow OH + O_2$		2.00×10^{13}	0.0	0.0	[17]
15. $HO_2 + OH \rightarrow H_2O + O_2$		2.89×10^{13}	0.0	−2.1	[16]
		Hydrogen peroxide reactions			
16.[g] $OH + OH + M \rightarrow H_2O_2 + M$	k_0	2.30×10^{18}	−0.9	−7.1	See text
	k_∞	7.40×10^{13}	−0.4	0.0	
17. $HO_2 + HO_2 \rightarrow H_2O_2 + O_2$		3.02×10^{12}	0.0	5.8	[13]
18. $H_2O_2 + H \rightarrow HO_2 + H_2$		4.79×10^{13}	0.0	33.3	[13]
19. $H_2O_2 + H \rightarrow H_2O + OH$		1.00×10^{13}	0.0	15.0	[13]
20. $H_2O_2 + OH \rightarrow H_2O + HO_2$		7.08×10^{12}	0.0	6.0	[13]
21. $H_2O_2 + O \rightarrow HO_2 + OH$		9.63×10^{6}	2.0	16.7	[13]
		Conversion of CO to CO_2			
22. $CO + OH \rightarrow CO_2 + H$		4.40×10^{6}	1.5	−3.1	[10]
23. $CO + HO_2 \rightarrow CO_2 + OH$		6.00×10^{13}	0.0	96.0	[10]
24. $CO + O_2 \rightarrow CO_2 + O$		1.00×10^{12}	0.0	199.4	See text
		Formyl reactions			
25.[h] $HCO + M \rightarrow CO + H + M$		1.86×10^{17}	−1.0	71.1	[18]
26. $HCO + H \rightarrow CO + H_2$		1.00×10^{14}	0.0	0.0	[10]
27. $HCO + O \rightarrow CO + OH$		3.00×10^{13}	0.0	0.0	[10]
28. $HCO + O \rightarrow CO_2 + H$		3.00×10^{13}	0.0	0.0	[10]
29. $HCO + OH \rightarrow CO + H_2O$		5.02×10^{13}	0.0	0.0	[10]
30. $HCO + O_2 \rightarrow CO + HO_2$		3.00×10^{13}	0.0	0.0	[10]

[a] Specific reaction-rate constant $k = AT^n e^{-E/R^0 T}$; units mol/cm^3, s^{-1}, K, kJ/mol.
[b] Chaperon efficiencies are 2.5 for H_2, 12.0 for H_2O, 1.9 for CO, 3.8 for CO_2, 0.5 for Ar and He, and 1.0 for all other species.
[c] Chaperon efficiencies are 2.5 for H_2, 12.0 for H_2O, 1.9 for CO, 3.8 for CO_2, 0.4 for Ar and He, and 1.0 for all other species.
[d] Chaperon efficiencies are 2.5 for H_2, 12.0 for H_2O, 1.9 for CO, 3.8 for CO_2, 0.2 for Ar and He, and 1.0 for all other species.
[e] Chaperon efficiencies are 2.5 for H_2, 12.0 for H_2O, 1.9 for CO, 3.8 for CO_2, 0.7 for Ar and He, and 1.0 for all other species.
[f] Chaperon efficiencies are 2.5 for H_2, 16.0 for H_2O, 1.2 for CO, 2.4 for CO_2, 0.7 for Ar and He, and 1.0 for all other species; Troe falloff with $F_c = 0.5$.
[g] Chaperon efficiencies are 2.0 for H_2, 6.0 for H_2O, 1.5 for CO, 2.0 for CO_2, 0.4 for Ar and He, and 1.0 for all other species; Troe falloff with $F_c = 0.265\exp(-T/94\ \mathrm{K}) + 0.735\exp(-T/1756\ \mathrm{K}) + \exp(-5182\ \mathrm{K}/T)$.
[h] Chaperon efficiencies are 1.9 for H_2, 12.0 for H_2O, 2.5 for CO, 2.5 for CO_2, and 1.0 for all other species.

again for all steps, and certain revisions were made on the basis of more recent literature and to obtain the agreements seen in Figs. 1 and 2.

The rate of the recombination step 6, $H + OH + M \rightarrow H_2O + M$, was increased by about 80% to reduce high-temperature hydrogen–air burning veloci-

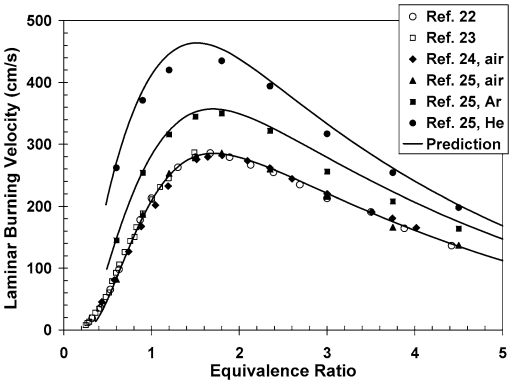

Fig. 1. Measured and predicted laminar burning velocities of hydrogen–oxygen-inert flames at 1 atm and initially at 298 K with a dilution factor $f = 0.214$, for inert nitrogen (air), argon, and helium.

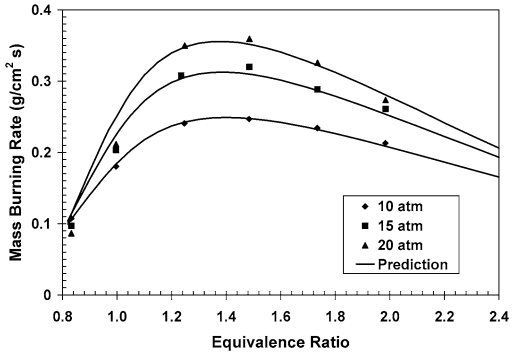

Fig. 2. Measured [24] and predicted laminar mass burning rates of hydrogen–oxygen-helium mixtures with a dilution factor $f = 0.08$, initially at 298 K, for pressures from 10 to 20 atm.

ties, on the basis of newer literature [28–30], which supports this revision, the listed rate being an average of the rates in the newer literature. The rate of step 11, $HO_2 + H \rightarrow 2OH$, had been decreased to reduce predicted propane–air burning velocities [1], improving agreements, and that similarly helps for hydrogen–air flames. Associated with this decrease, considerations of rate and branching-ratio results [31,32] prompted recommending a corresponding reduction in the rate of step 12, $HO_2 + H \rightarrow H_2 + O_2$ [15]. The specific reaction-rate constant

$$k = AT^n e^{-E/RT}$$

with the recommended [15] parameter values listed as entry 12 in Table 1 is therefore now adopted for this step, improving agreements slightly for both burning velocities and autoignition times. Revision of the rate of step 17, $2HO_2 \rightarrow H_2O_2 + O_2$, was considered but rejected as not well justified at the high temperatures of interest.

All of the other changes that were made pertain to the three-body recombinations. Newer [13] rate parameters were adopted for $O + H + M \rightarrow OH + M$ (entry 8 of Table 1) with the recommended chaperon efficiencies. The rate parameters for $O + O + M \rightarrow O_2 + M$ (entry 7) also were taken from this reference, although chaperon efficiencies of 0.2 were introduced for argon and helium to avoid employing separate reactions for these third bodies, the selected value representing an average over the temperature range of interest here (1000 to 2500 K). All rate parameters are written consistently with a chaperon efficiency of unity for nitrogen. For step 5, $H + H + M \rightarrow H_2 + M$, the recommendation of Baulch et al. [16] was adopted; these authors give values only for argon as the chaperon, whose efficiency with respect to nitrogen was assumed to be 0.5, slightly improving fuel-rich burning-velocity agreements in Fig. 1 and resulting in rates that lie between those of Li [26] and of the optimized mechanism of Davis et al. [30], whose common relative efficiencies [26,30] were adopted. For reaction 9, $O + OH + M \rightarrow HO_2 + M$, chaperon efficiencies are now introduced which are the same as those of $O + H + M \rightarrow OH + M$, while the rate is slightly reduced (by 20%) from our previous value [33]. The Troe [34] rate parameters and falloff recommendations for step 10, $H + O_2 + M \rightarrow HO_2 + M$, for nitrogen as the bath gas (e.g., $F_c = 0.5$) were adopted, improving both burning-velocity agreement for high-pressure experiments with helium dilution and ignition-time agreement; Petrova and Williams [1] have a misprint in k_0 for this step. To avoid having to introduce either a different rate expression or temperature-dependent chaperon efficiencies for argon as the bath gas for this reaction, just as was done for the other recombination processes discussed above, constant chaperon efficiencies were selected, a high value for water being used for agreement with measured autoignition times and diffusion-flame extinction by water addition, and a value for argon being selected consistent with autoignition times. Finally, for step 16, $OH + OH + M \rightarrow H_2O_2 + M$, the listed rate parameters [9] are obtained from those for nitrogen of Baulch et al. [35] (who write the reaction in the opposite direction) by use of equilibrium constants, but the argon efficiency was decreased from 0.7 to 0.4, a better average, between 1000 and 2500 K, of the temperature-dependent recommendation of Baulch et al. [35].

3. Hydrogen diffusion-flame extinction

The mechanism with these updated rate parameters also was tested against counterflow diffusion-flame extinction experiments. Comparisons are shown

in Figs. 3 and 4. The extinction strain-rate data in Fig. 3 [36] are seen to lie below the solid curve, calculated using CHEMKIN 3.7 OPDIFF with complete transport. Since there is an indication of inaccurate transport data for hydrogen (as well as helium) in the code [37], for comparison purposes the calculation also was performed with the Soret effects excluded, to obtain an idea of how important light-species transport may be. The results, shown by the dashed curve, agree better with the data, about as good as the agreement obtained [36] with an early version of the present mechanism. In view of the nonnegligible influences of transport uncertainties for these experiments, until improved transport properties for hydrogen and helium can be incorporated into the computations, the agreement with the updated mechanism is considered acceptable.

Fig. 4 tests the influence of water addition on the extinction strain rate, employing data [38] against

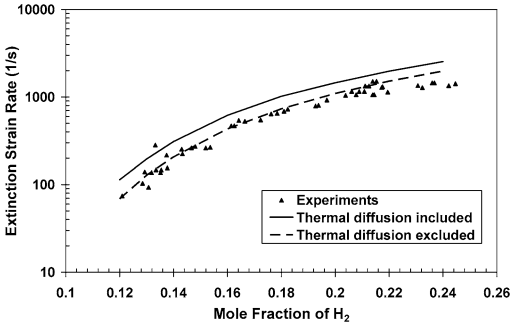

Fig. 3. Measured [36] and predicted extinction strain rate as a function of the mole fraction of hydrogen in a hydrogen–nitrogen fuel mixture for a counterflow diffusion flame of the diluted fuel and air.

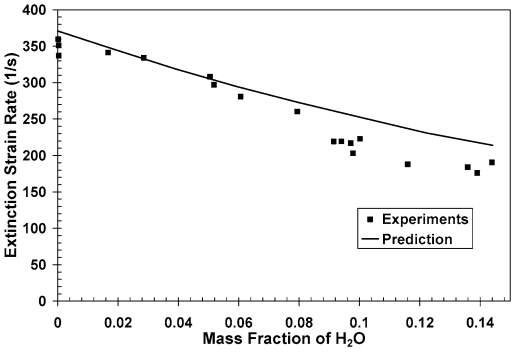

Fig. 4. Measured [38] and predicted extinction strain rate as a function of the mass fractions of water in the oxidizer stream for a counterflow diffusion flame having a hydrogen–nitrogen mixture at room temperature as fuel (hydrogen mole fractions between 0.28 and 0.29) and an oxygen–nitrogen–water mixture at 383 K (dilution f approximately 0.1) as oxidizer.

which other mechanisms have been tested earlier. The agreement seen in this figure is somewhat better than found earlier [38], largely as a consequence of the increased chaperon efficiency for water in the 10, $H + O_2 + M \rightarrow HO_2 + M$, which decreases the extinction strain rate with increasing water concentrations more rapidly than predicted earlier. Although even better agreement can be obtained with falloff [39] for H_2O different than that for N_2, it was preferred to accept the agreement shown for the sake of not having to treat the reaction with H_2O as a separate reaction.

4. Burning velocities of carbon monoxide

Since flames of carbon monoxide are dominated by hydrogen chemistry in practice, it is necessary only to add the three species CO, CO_2, and HCO, along with nine additional reversible elementary steps, to the hydrogen–oxygen mechanism, to obtain a workable 30-step mechanism among 11 species for the combustion of carbon monoxide, as seen in Table 1. Fig. 5 tests predictions of this mechanism against recent burning-velocity data as a function of equivalence ratio for two different mixtures of hydrogen and carbon monoxide in air [40]. Fig. 6 similarly tests the dependence on the fraction of carbon monoxide in the fuel for stoichiometric mixtures [40]. The excellent agreement in these two figures indicates that slightly revised rate parameters for step 22, $CO + OH \rightarrow CO_2 + H$ [26], and revised rate parameters for step 23, $CO + HO_2 \rightarrow CO_2 + OH$ [41], motivated mainly by experiments at temperatures lower than those of interest here, are unnecessary for the present purposes; it was sufficient to retain the earlier [10] rates unchanged, which agree with results of a recent optimized mechanism [30].

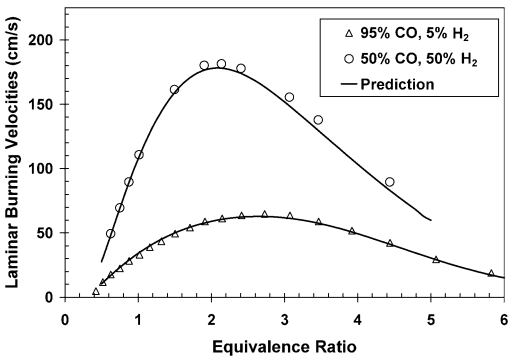

Fig. 5. Measured [40] and predicted laminar burning velocities as functions of the equivalence ratio for two different mixtures of hydrogen and carbon monoxide in air at 1 atm and initially at 298 K.

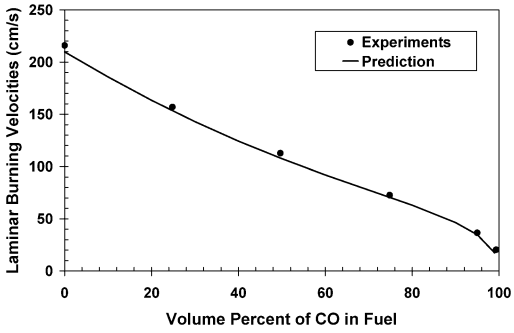

Fig. 6. Measured [40] and predicted laminar burning velocities of stoichiometric fuel–air mixtures at 1 atm and initially at 298 K, as a function of the percentage of carbon monoxide in a fuel consisting of a mixture of hydrogen and carbon monoxide.

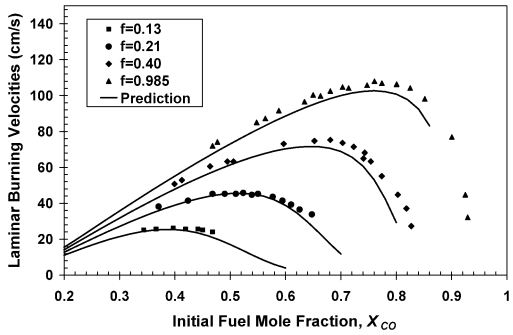

Fig. 7. Measured [42] and predicted laminar burning velocities at 1 atm and initially at 298 K, as functions of the initial fuel mole fraction of carbon monoxide X_{CO} at various dilutions f, for flames of carbon monoxide with initial hydrogen mole fraction $X_{H_2} = 0.015(X_{CO} + X_{H_2} + X_{H_2O})$.

An earlier version of the mechanism was tested previously [11] for flames of carbon monoxide with trace amounts of hydrogen and water. Fig. 7 repeats that test with the updated mechanism and exhibits agreements no worse than before.

5. Autoignition of carbon monoxide

The mechanism has not been tested previously for autoignition of mixtures of carbon monoxide and hydrogen, even though there are shock-tube data [43,44] on which such tests can be made. These tests were performed here using the homogeneous, adiabatic, isochoric option of CHEMKIN 3.7 AURORA. Fig. 8 shows comparisons with one set of data [43] based on three different definitions of ignition times, all derived from profiles of the measured concentration of carbon dioxide. Fig. 9 shows comparisons with another set of data [44] at lower pressure, based on a different ignition-time criterion. In all comparisons,

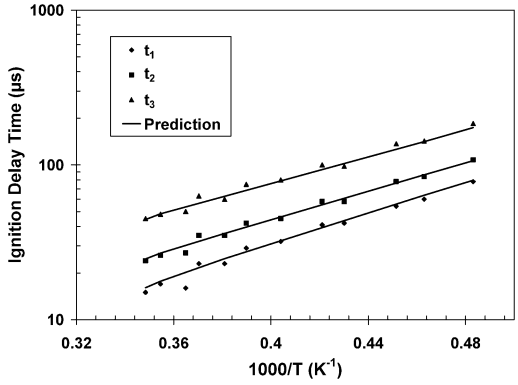

Fig. 8. Measured [43] and predicted ignition times of a mixture of 12.15% CO, 0.05% H_2, 1.0% O_2, and 86.8% Ar by volume at pressures between 1.4 and 2.2 atm, according to three different definitions of the ignition times based on concentration–time profiles of carbon dioxide, namely, the time t_1 of the zero intercept of the maximum-slope straight line, the time t_2 at which the concentration is 10^{16} molecules/cm^3, and the time t_3 at which the concentration is 3×10^{16} molecules/cm^3.

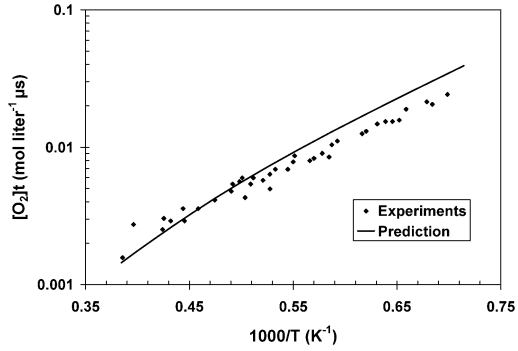

Fig. 9. Measured [44] and predicted ignition times, defined as hydroxyl concentrations reaching 2.5×10^{-10} mol/cm^3, for a mixture of 3% CO, 1% H_2, 5% O_2, and 91% Ar by volume, at pressures between 0.15 and 0.30 atm.

the computational and experimental ignition-time criteria are the same. The agreements are comparable with or better than those obtained [1,4,5] for other fuels; they are excellent in Fig. 8, while the predicted slope is a little higher than the average experimental data in Fig. 9. The experiments in this last figure were performed over a range of pressures, with values of the pressure not specified for each specific data point, and for each point it is possible to select a value of the pressure within the range that produces agreement between the prediction and the measurement. It is unclear whether the noticeably greater theoretical slope, which agrees with the slope of Li [26], should be attributable to erroneous values of rate parameters or to systematic experimental error, which becomes more

difficult to avoid at these low pressures in shock tubes of the dimensions employed.

It was found that although step 24, $CO + O_2 \rightarrow CO_2 + O$, has no measurable influences on burning velocities and had not been retained previously as part of the mechanism, it does have a noticeable influence on these ignition times at low hydrogen content, contributing to initiation. This step therefore is now added to the mechanism, with rate parameters giving half the rate recommended by Tsang and Hampson [45]. This selection improves agreements somewhat in Fig. 8 and lies in the range of other values in the literature, even lower rates having been reported [46].

6. Conclusions

The present study has led to a few revisions of rate parameters for elementary steps in the mechanism for hydrogen and to deletion of a hydrogen initiation step and addition of an initiation step for carbon monoxide. Small increases in three-body recombination rates for certain steps and some changes in chaperon efficiencies were identified. With these alterations, reasonable agreement is obtained with available measured burning velocities, diffusion-flame extinction conditions, and autoignition times. The submechanism for hydrogen and carbon monoxide appearing in Table 1 thus is judged acceptable for use in future studies.

Acknowledgment

This work was supported by the National Science Foundation through Grant CTS 0129562.

References

[1] M.V. Petrova, F.A. Williams, Combust. Flame (2005), in press.
[2] S.C. Li, F.A. Williams, Combust. Flame 118 (1999) 399–414.
[3] M.M.Y. Waly, S.C. Li, F.A. Williams, J. Eng. Gas Turbine Power 122 (2000) 651–658.
[4] B. Varatharajan, F.A. Williams, J. Propul. Power 18 (2002) 344–351.
[5] M.M.Y. Waly, S.C. Li, F.A. Williams, Proc. Combust. Inst. 28 (2000) 2005–2012.
[6] B. Varatharajan, F.A. Williams, Combust. Flame 124 (2001) 624–645.
[7] S.C. Li, F.A. Williams, Proc. Combust. Inst. 26 (1996) 1017–1024.
[8] S.C. Li, F.A. Williams, Proc. Combust. Inst. 27 (1998) 485–493.
[9] G. Del Alamo, F.A. Williams, A.L. Sanchez, Combust. Sci. Technol. 176 (2004) 1599–1626.
[10] M.L. Rightley, F.A. Williams, Combust. Sci. Technol. 125 (1997) 181–200.
[11] M.L. Rightley, F.A. Williams, Combust. Flame 101 (1995) 287–301.
[12] D.A. Masten, R.K. Hanson, C.T. Bowman, J. Phys. Chem. 94 (1990) 7119–7128.
[13] R.A. Yetter, F.L. Dryer, H. Rabitz, Combust. Sci. Technol. 79 (1991) 97–128.
[14] M.D. Smooke, J. Comput. Phys. 48 (1982) 72–105.
[15] M.A. Mueller, T.J. Kim, R.A. Yetter, F.L. Dryer, Int. J. Chem. Kinet. 31 (1999) 113–125.
[16] D.L. Baulch, C.J. Cobos, R.A. Cox, C. Esser, P. Frank, Th. Just, J.A. Kerr, M.J. Pilling, J. Troe, R.W. Walker, J. Warnatz, J. Phys. Chem. Ref. Data 21 (1992) 411–734.
[17] J. Warnatz, in: W.C. Gardiner (Ed.), Combustion Chemistry, Springer-Verlag, Berlin, 1984, pp. 197–360.
[18] R.P. Lindstedt, G. Skevis, Combust. Sci. Technol. 125 (1997) 73–137.
[19] R.J. Kee, F.M. Rupley, J.A. Miller, M.E. Coltrin, J.F. Grcar, E. Meeks, H.K. Moffat, A.E. Lutz, G. Dixon-Lewis, M.D. Smooke, J. Warnatz, G.H. Evans, R.S. Larson, R.E. Mitchell, L.R. Petzold, W.C. Reynolds, M. Caracotsios, W.E. Stewart, P. Glarborg, C. Wang, O. Adigun, W.G. Houf, C.P. Chou, S.F. Miller, CHEMKIN Collection, Release 3.7.1, Reaction Design, San Diego, CA, 2003.
[20] H. Pitsch, M.S. thesis, RWTH Aachen, Germany, 1993.
[21] G. Balakrishnan, F.A. Williams, J. Propul. Power 10 (1994) 434–437.
[22] D.R. Dowdy, D.B. Smith, S.C. Taylor, A. Williams, Proc. Combust. Inst. 23 (1990) 325–332.
[23] F.N. Egolfopoulos, C.K. Law, Proc. Combust. Inst. 23 (1990) 333–340.
[24] S.D. Tse, D.L. Zhu, C.K. Law, Proc. Combust. Inst. 28 (2000) 1793–1800.
[25] O.C. Kwon, G.M. Faeth, Combust. Flame 124 (2001) 590–610.
[26] J. Li, Ph.D. thesis, Princeton University, 2004.
[27] J.V. Michael, J.W. Sutherland, L.B. Harding, A.F. Wagner, Proc. Combust. Inst. 28 (2000) 1471–1478.
[28] J. Li, Z. Zhao, A. Kazakov, F.L. Dryer, Int. J. Chem. Kinet. 36 (2004) 566–575.
[29] O.M. Conaire, H.J. Curran, J.M. Simmie, W.J. Pitz, C.K. Westbrook, Int. J. Chem. Kinet. 36 (2004) 603–622.
[30] S.G. Davis, A.V. Joshi, H. Wang, F. Egolfopoulos, Proc. Combust. Inst. 30 (2005) 1283–1292.
[31] H. Hippler, J. Troe, J. Willner, J. Chem. Phys. 93 (1990) 1755–1760.
[32] R.R. Baldwin, M.E. Fuller, J.S. Hillman, D. Jackson, R.W. Walker, Trans. Faraday Soc. 70 (1974) 635–641.
[33] E. Gutheil, G. Balakrishnan, F.A. Williams, in: N. Peters, B. Rogg (Eds.), Reduced Kinetic Mechanisms for Applications in Combustion Systems, Springer-Verlag, Berlin, 1993, Chap. 11.
[34] J. Troe, Proc. Combust. Inst. 28 (2000) 1463–1469.
[35] D.L. Baulch, C.J. Cobos, R.A. Cox, C. Esser, P. Frank, Th. Just, J.A. Kerr, M.J. Pilling, J. Troe, R.W. Walker, J. Warnatz, J. Phys. Chem. Ref. Data 23 (1994) 847–1033.

[36] G. Balakrishnan, D. Trees, F.A. Williams, Combust. Flame 98 (1994) 123–126.
[37] P. Paul, J. Warnatz, Proc. Combust. Inst. 27 (1998) 495–504.
[38] R. Seiser, K. Seshadri, Proc. Combust. Inst. 30 (2005) 407–414.
[39] R.W. Bates, D.M. Golden, R.K. Hanson, C.T. Bowman, Phys. Chem. Chem. Phys. 3 (2001) 2337–2342.
[40] I.C. McLean, D.B. Smith, S.C. Taylor, Proc. Combust. Inst. 25 (1994) 749–757.
[41] M.A. Mueller, R.A. Yetter, F.L. Dryer, Int. J. Chem. Kinet. 31 (1999) 705–724.
[42] B. Lewis, G. von Elbe, Combustion, Flames, and Explosions of Gases, third ed., Academic Press, New York, 1987, p. 398.
[43] A.M. Dean, D.C. Steiner, E.E. Wang, Combust. Flame 32 (1978) 73–83.
[44] W.C. Gardiner, M. McFarland, K. Morinaga, T. Takeyama, B.F. Walker, J. Phys. Chem. 75 (1971) 1504–1509.
[45] W. Tsang, R.F. Hampson, J. Phys. Chem. Ref. Data 15 (1986) 1087–1276.
[46] A.M. Dean, G.B. Kistiakowsky, J. Chem. Phys. 54 (1971) 1718–1725.